Neuron 56, 717–727, June 7, 2007 ©2007 Elsevier Inc. DOI 10.1016/j.neuron.2007.08.032

Tandem-Pore K^+ Channels Mediate Inhibition of Orexin Neurons by Glucose

Denis Burdakov,[1,*] Lise T. Jensen,[2] Haris Alexopoulos,[3] Rhiannan H. Williams,[1] Ian M. Fearon,[1] Ita O'Kelly,[1] Oleg Gerasimenko,[4] Lars Fugger,[2,5] and Alexei Verkhratsky[1]

[1] Faculty of Life Sciences
University of Manchester
Oxford Road
Manchester M13 9PT
United Kingdom

[2] Department of Clinical Immunology
Aarhus University Hospital
Skejby Sygehus
Denmark

[3] University Laboratory of Physiology
University of Oxford
United Kingdom

[4] Physiological Laboratory
University of Liverpool
United Kingdom

[5] MRC Human Immunology Unit and Department of Clinical Neurology
Weatherall Institute of Molecular Medicine
John Radcliffe Hospital
University of Oxford
United Kingdom

Summary

Glucose-inhibited neurons orchestrate behavior and metabolism according to body energy levels, but how glucose inhibits these cells is unknown. We studied glucose inhibition of orexin/hypocretin neurons, which promote wakefulness (their loss causes narcolepsy) and also regulate metabolism and reward. Here we demonstrate that their inhibition by glucose is mediated by ion channels not previously implicated in central or peripheral glucose sensing: tandem-pore K^+ (K_{2P}) channels. Importantly, we show that this electrical mechanism is sufficiently sensitive to encode variations in glucose levels reflecting those occurring physiologically between normal meals. Moreover, we provide evidence that glucose acts at an extracellular site on orexin neurons, and this information is transmitted to the channels by an intracellular intermediary that is not ATP, Ca^{2+}, or glucose itself. These results reveal an unexpected energy-sensing pathway in neurons that regulate states of consciousness and energy balance.

Introduction

A fundamental aspect of animal survival is the ability to react appropriately to changes in life-sustaining energy supplies. In mammals, the brain plays a central role in these vital adaptations, detecting changes in body energy levels and initiating coordinated adjustments in behavior and metabolism (Saper et al., 2002; Schwartz et al., 2000). One of the earliest explanations for how the brain monitors body energy levels came from the discovery of "glucose-sensing" hypothalamic neurons, which respond to rises in ambient glucose levels with increases (glucose-excited cells) or decreases (glucose-inhibited cells) in firing rate (Anand et al., 1964; Oomura et al., 1969). These cells are critical for responding to the ever-changing body energy state with finely orchestrated changes in arousal, food seeking, hormone release, and metabolic rate, to ensure that the brain always has adequate glucose (Levin et al., 1999; Routh, 2002; Burdakov et al., 2005b). It is therefore important to understand how glucose exerts its effects on these neurons.

For most glucose-excited cells, there is now strong evidence that the excitation involves intracellular glucose entry and closure of ATP-sensitive K^+ channels (Ashford et al., 1990; Routh, 2002). In contrast, the biophysical nature of glucose-mediated inhibition (glucose inhibition) is a long-standing mystery. It has been speculated that glucose inhibition may involve enhanced activity of either the sodium pump (Oomura et al., 1974) or chloride channels (Routh, 2002). However, ion substitution experiments necessary to test these theories have not been performed. Moreover, even the basic site of glucose action (intracellular versus extracellular) in glucose-inhibited neurons is unknown.

Among glucose-inhibited cells are neurons containing the recently described transmitters orexins/hypocretins (orexin neurons) (Sakurai et al., 1998; de Lecea et al., 1998). These cells are highly important regulators of states of consciousness. They project to all major brain areas except the cerebellum, with prominent innervation of key arousal and autonomic regions, where orexins are released and act on specific G protein-coupled receptors (OX_1R and OX_2R) (Marcus et al., 2001; Peyron et al., 1998; Sakurai et al., 1998; Willie et al., 2001; Sutcliffe and de Lecea, 2002). Defects in orexin signaling result in narcolepsy, demonstrating that orexin neurons are vital for sustaining normal wakefulness (Chemelli et al., 1999; Lin et al., 1999; Peyron et al., 2000; Thannickal et al., 2000; Sutcliffe and de Lecea, 2002). The activity of orexin neurons also regulates appetite and metabolic rate, and loss of orexin neurons leads to obesity (Hara et al., 2001). Moreover, key roles for orexin neurons are emerging in learning, reward seeking, and addiction (Selbach et al., 2004; Harris et al., 2005; Smith and Pang, 2005; Borgland et al., 2006).

Considering these crucial roles of orexin neurons, their recently described inhibition by glucose (Yamanaka et al., 2003; Burdakov et al., 2005a) is likely to have considerable implications for the regulation of states of consciousness and energy balance. However, as in other glucose-inhibited neurons, it is unknown how glucose suppresses the electrical activity of orexin cells. Because the sensitivity of orexin cell firing to the small changes in extracellular glucose that occur between normal meals has never been tested, the daily physiological relevance of their glucose sensing is also unknown.

*Correspondence: dib22@cam.ac.uk

To address these important unknowns, here we identify orexin neurons via targeted expression of GFP in transgenic mice and document key properties of their inhibition by glucose. We demonstrate that glucose inhibition is mediated by activation of "leak" K^+ (K_{2P}) channels (also known as tandem-pore or two-pore domain K^+ channels), which were not previously implicated in central or peripheral glucose sensing. Crucially, this electrical mechanism allows orexin neurons to encode minute changes in glucose levels reflecting physiological variations occurring in the brain between normal meals. Glucose-modulated K_{2P} channels are activated by extracellular, but not intracellular, application of glucose. Together, these results identify an unexpected physiological role for the recently characterized K_{2P} channels and shed light on the long-elusive mechanism of glucose inhibition, thus providing new insights into cellular pathways regulating vigilance states and energy balance.

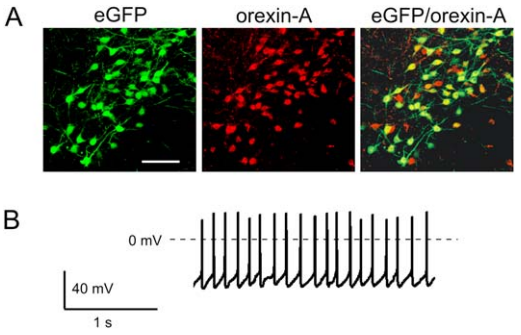

Figure 1. Properties of eGFP-Expressing Neurons from Orexin-eGFP Mice

(A) Imaging of eGFP (green) and immunolabeled orexin-A (red). Colocalization of eGFP and orexin-A is shown in yellow. Scale bar, 100 μm.

(B) Current-clamp recording from an orexin-eGFP neuron showing intrinsic activity.

Results

Identifying Living Orexin Neurons via Targeted Expression of eGFP

To identify living orexin neurons in situ, we made transgenic mice in which the expression of enhanced green fluorescent protein (eGFP) is driven by the human *prepro-orexin* promoter (orexin-eGFP mice; see Experimental Procedures). This proved to be a highly reliable marker of orexin cells: up to 80% of orexin-containing neurons in brain slices from orexin-eGFP mice were labeled with eGFP, as in previous studies of eGFP expression driven by this promoter (Li et al., 2002; Yamanaka et al., 2003). Expression of orexin in 100% of eGFP neurons (Figure 1A) was further confirmed by scanning individual cells (n = 70) at high magnification.

To study electrical activity of orexin neurons, we performed whole-cell patch-clamp recordings in acutely isolated brain slices. Exactly like wild-type mouse orexin neurons (Burdakov et al., 2005a), eGFP-containing neurons exhibited spontaneous electrical activity (Figure 1B; n = 20) and were inhibited when the extracellular solution was switched from 0.2 to 4.5 mM glucose (Figure 2A, n = 19/20). This confirmed that transgenic eGFP expression does not disrupt intrinsic electrophysiology and glucose sensing of mouse orexin neurons, which is also suggested by previous reports (Li et al., 2002; Yamanaka et al., 2003).

Biophysical Identity of the Current Responsible for Glucose Inhibition

To address the ionic nature of glucose inhibition, we combined intracellular ion substitutions with whole-cell recordings. First, we used a K-gluconate intracellular solution; in its presence, glucose induced hyperpolarization (Figure 2A). With this solution, the current responsible for hyperpolarization can be carried by two ions, K^+ and Cl^-, since only these ions have equilibrium (Nernst) potentials (E_{ion}) that are more negative than resting membrane potentials of orexin cells (E_K = −103 mV, E_{Cl} = −58 mV). This indicates that glucose inhibition is mediated by K^+ or Cl^- currents.

Next, we used a KCl intracellular solution (which was also used in all subsequent experiments). This solution sets E_{Cl} to ~0 mV, making K^+ channels the only ion channels that can hyperpolarize resting potentials of orexin cells. Under these conditions, glucose still produced pronounced hyperpolarization (Figure 2A, n = 38/41). This indicates that a K^+, and not Cl^-, current is responsible. Thus, the net glucose-induced current should have an equilibrium potential corresponding to E_K. We isolated the net glucose-induced current by subtracting whole-cell currents in 0.2 mM extracellular glucose from those recorded from the same cell in 4.5 mM glucose (Figures 2A and 2B). Glucose-induced current (Figure 2C) had an equilibrium potential of −104 ± 1 mV (n = 30), confirming its high selectivity for K^+ ions (E_K = −103 mV). Direct injections of currents of similar size into orexin neurons mimicked hyperpolarization produced by glucose (Figure 2F), confirming that the glucose-induced current was large enough to account for glucose inhibition.

The K^+ channel families fall into three groups based on voltage and Ca^{2+} dependence of their currents: (1) voltage- and/or Ca^{2+}-gated channels, (2) inwardly rectifying channels, and (3) leak channels exhibiting Goldman-Hodgkin-Katz (GHK) outward rectification (Hille, 2001). To determine which of these channel families mediates glucose inhibition, we focused on the current-voltage (I-V) relationship of the net glucose-induced current (Figure 2C). This showed clear outwardly rectifying behavior that was well described by the GHK current equation (Figure 2C). This is strongly indicative of a leak K^+ conductance lacking intrinsic voltage dependence, whereas K^+ channels of types (1) and (2) (above) have strikingly different I-V relationships (Hille, 2001).

Glucose-induced current was also unaffected by fixing cytosolic [Ca^{2+}] at 90 nM with an intracellularly applied BAPTA-Ca^{2+} mixture (n = 15, see Figure 7D and associated text), providing a further strong argument against involvement of Ca^{2+}-activated K^+ currents (Gribkoff et al., 2001). Overall, the properties of glucose-induced currents were thus consistent with leak K^+ channels but not with other K^+ channel families. Analyzing the time course of net glucose-induced currents evoked in response to voltage steps revealed rapid activation and minimal time-dependent decay (Figures

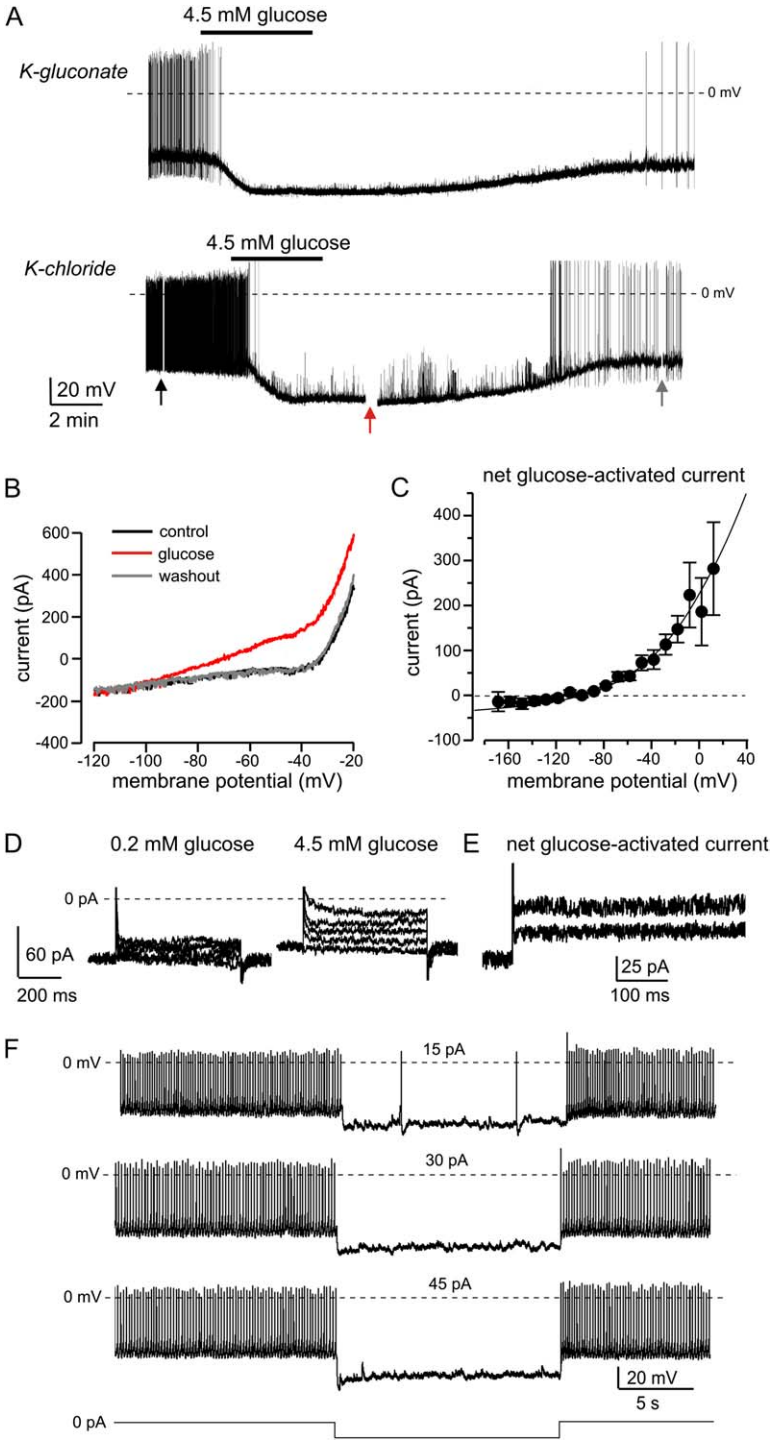

Figure 2. Biophysical Properties of Glucose-Activated Current in Orexin Neurons

(A) Effects of elevating extracellular glucose from 0.2 to 4.5 mM on membrane potential with K-gluconate (top) and K-chloride (bottom) pipette solutions. Arrows indicate when currents shown in (B) were recorded.

(B) Effects of glucose on membrane I-V relationship of the cell in (A).

(C) I-V plot of net glucose-activated current (n = 6). The line is a fit of the GHK equation to the data (see Experimental Procedures for fitting parameters). Data are means ± SEM.

(D) Effects of glucose on membrane currents obtained with voltage steps. Currents were produced by steps to −80, −70, −60, and −50 mV (from −90 mV).

(E) Time course of activation and inactivation of net glucose-activated currents (high glucose minus low glucose), obtained by steps to −70 and −60 mV (from −90 mV).

(F) Effects of current injections on an orexin cell: 15 (top), 30 (middle), and 45 (bottom) pA (the current-clamp protocol is shown schematically below).

2D and 2E). These kinetic features are further typical attributes of leak K^+ channels (Goldstein et al., 2001).

Modulation of Glucose-Induced Currents by Halothane and Acid

Together, the K^+ selectivity, GHK outward rectification, rapid activation, and minimal inactivation indicated the involvement of K^+-selective leak channels. In mammals, such leak K^+ channels are made up of K_{2P} protein subunits, encoded by the KCNK gene family (Lesage and Lazdunski, 2000; Patel and Honore, 2001; Goldstein et al., 2001). This family has 15 genes, most of which produce functional ion channels upon expression (Goldstein et al., 2005). Different subfamilies of these K_{2P} channels exhibit different responses to certain modulators. Notably, halothane activates K_{2P} channels belonging to "TASK" or "TREK" subfamilies, but inhibits channels of "THIK" and "TALK" subfamilies (reviewed in O'Connell et al., 2002). Of these, TASK K_{2P} channels are potently inhibited by extracellular acid, which,

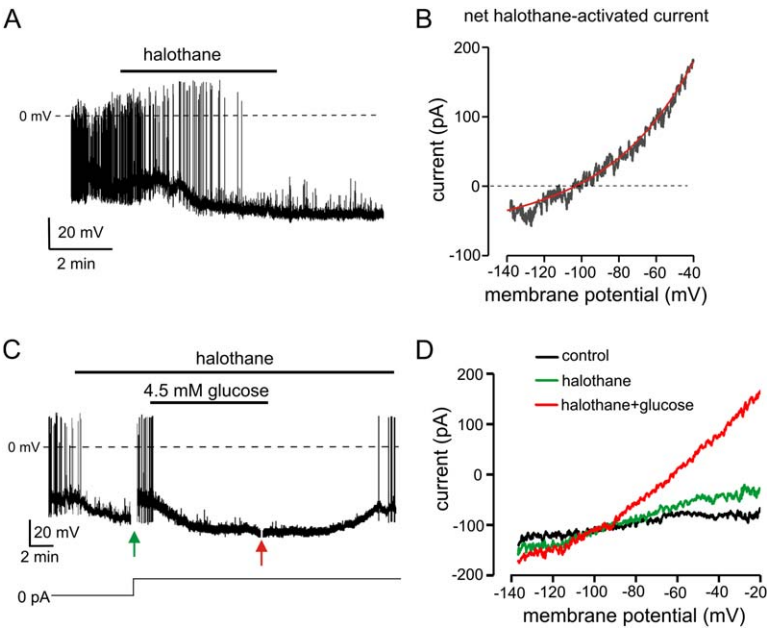

Figure 3. Effects of Halothane on Orexin Neurons

(A) Effect of halothane (1%) on membrane potential.

(B) I-V relationship of net halothane-induced current from cell shown in (A). The red line is a fit of the GHK equation to the data.

(C) Effect of glucose in the presence of halothane (1%). The cell was first hyperpolarized by halothane, then returned to prehalothane potential by current injection (the current-clamp protocol is shown below the trace). Arrows indicate when the currents shown in (D) were recorded.

(D) Effects of halothane and glucose on membrane I-V relationship of the cell shown in (C).

together with activation by halothane and GHK rectification, is among the best diagnostic tests for TASK K_{2P} channels (Bayliss et al., 2003).

In our experiments, halothane (1%, based on Meuth et al., 2003) mimicked actions of glucose on the membrane potential (Figure 3A, n = 5), an effect that was not readily reversed in our slice preparations. The net halothane-induced currents were identical to glucose-induced currents in GHK rectification (Figure 3B), activation/inactivation kinetics (data not shown), and reversal potentials (−104 ± 3 mV), in four out of six cells. In the remaining two cells (which were not used for analysis), halothane-induced current reversed at potentials positive to E_K (−80 and −75 mV), indicating that, in some orexin cells, halothane also modulates other ion currents, as reported for other neurons (Meuth et al., 2003). To examine the actions of glucose in the presence of halothane, halothane-hyperpolarized cells were returned to control (prehalothane) membrane potentials by current injection (Figure 3C). Subsequent glucose application still induced hyperpolarization and further activated the halothane-induced current (Figures 3C and 3D, n = 5), regardless of whether the halothane-activated currents were large or small. This indicated that halothane did not fully activate the current, consistent with previous data showing that halothane cannot by itself attain the maximal open state of K_{2P} channels (Sirois et al., 2000). Overall, these effects of halothane implicated either TASK or TREK K_{2P} channels.

We next tested the effect of extracellular acid, which clearly reversed the effects of glucose on the membrane potential and current of orexin cells (Figures 4A and 4B, n = 15). The net acid-inhibited currents were indistinguishable from glucose-induced currents in GHK rectification (Figure 4D, n = 7), reversal potentials (−102 ± 1, n = 7), and activation/inactivation kinetics (n = 5, data not shown). Extracellular acidification from pH 7.3 to 5.9 acted as a selective way of blocking glucose-activated channels, because at 0.2 mM of glucose (when glucose-activated channels are closed) acidification did not affect the membrane potential or currents (Figure 4C, n = 4). This allowed us to test whether impairing the function of glucose-activated channels with low extracellular pH would prevent glucose responses. On the background of pH 5.9, glucose failed to induce any changes in the membrane potential or currents of orexin cells (Figure 4C, n = 5). We confirmed that glucose-modulated channels were present in all of these cells by returning pH to the control value of 7.3; we first observed a rapid unmasking of glucose responses, followed by normal responses to further applications of glucose (Figure 4C, n = 5).

In summary, glucose-induced currents exhibit GHK outward rectification, inhibition by extracellular acid, and activation by halothane. Among cloned ion channels, TASK K_{2P} channels are at present unique in exhibiting this combination of attributes (Bayliss et al., 2003). Thus our data imply that TASK K_{2P} channels mediate glucose inhibition.

Evidence for TASK3 Subunits in Glucose-Activated Channels

We saw half-maximal inhibition (IC_{50}) of glucose-induced current at a pH of 6.9 (Figure 4E). This has implications for the channel identity, because different TASK channels have different sensitivities to acid, as illustrated by their IC_{50} pH values: ~7.3 for TASK1 (K_{2P}3.1), ~8.3 for TASK2 (K_{2P}5.1), ~6.7 for TASK3 (K_{2P}9.1), and ~10 for TASK4 (K_{2P}17.1) (reviewed in O'Connell et al., 2002). The measured value of 6.9 is closest to channels containing TASK3 subunits, such as TASK3 homomers or TASK3-containing heteromeric channels (Czirjak and Enyedi, 2002; O'Connell et al., 2002; Berg et al., 2004; Kang et al., 2004). However, the high variation of published IC_{50} values (e.g., Berg et al., 2004; Rajan et al., 2000) makes it difficult to rule out channels with a similar IC_{50}, e.g., TASK1, on the basis of acid sensitivity alone.

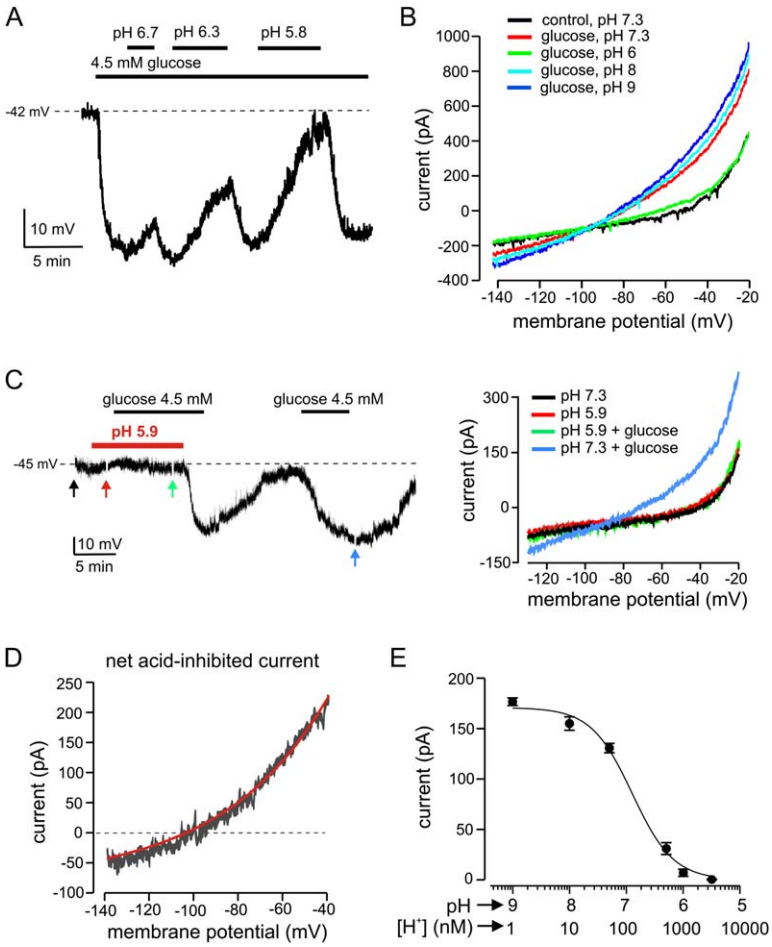

Figure 4. Effects of Extracellular pH on Glucose Responses of Orexin Neurons

(A) Effects of changes in pH on glucose-induced hyperpolarization.

(B) Effects of changes in pH on glucose-induced currents.

(C) Glucose does not affect membrane potential (left) and current (right) when pH is low (control extracellular solution is at a pH of 7.3).

(D) Net current inhibited by extracellular acidification (current at pH 7.3 minus current at pH 6, both in 4.5 mM glucose). The red line is a fit of the GHK equation to the data.

(E) Dose-response of acid-induced inhibition of glucose-activated currents (measured at −60 mV) (n = 5). The line is a fit of the Hill equation to the data (see Experimental Procedures), IC_{50} is at a pH 6.9. Data are means ± SEM.

Experiments performed in 1 μM tetrodotoxin.

Single-channel conductance provides a more accurate way of distinguishing TASK3-containing channels from TASK1 homomers (Bayliss et al., 2003; Kang et al., 2004). We measured single-channel activity using cell-attached recordings (with no glucose in the pipette; see Experimental Procedures). Glucose-activated channels were observed in six out of eight cell-attached patches (Figures 5A and 5B), but not in five out of five patches recorded using acidic (pH = 5.9) pipette solutions, as expected from whole-cell data (Figure 4). These channels exhibited flickering on-off kinetics typical of TASK channels (e.g., Kang et al., 2004; Leonoudakis et al., 1998) and had a conductance of 40 ± 1 pS (Figure 5C, n = 6 channels). This value is different from conductances of TASK1 homomers (~14 pS), but is in good agreement with TASK3-containing channels, which have conductances of 38.1 ± 0.7 pS (TASK3-containing heteromers) or 30–37.8 pS (TASK3 homomers) (Bayliss et al., 2003; Kang et al., 2004).

To distinguish between TASK3 homomers and TASK3-containing heteromers (which are biophysically identical), we used ruthenium red. It is well established that at 5–10 μM, this drug blocks TASK3 homomers by ~80%, but has little effect on TASK3-containing heteromers (Czirjak and Enyedi, 2002; Kang et al., 2004; Berg et al., 2004). We found no inhibitory effect of 10 μM ruthenium red on the glucose-induced current (Figure 5D, n = 4).

The pharmacological and biophysical profile of glucose-activated channels thus implicated heteromeric channels containing TASK3 subunits. In further corroboration of this conclusion, we detected TASK3 proteins in orexin neurons using two different antibodies (Figure 5E, n > 20 for each antibody; antibodies are described in Experimental Procedures). This is in agreement with high levels of TASK3 mRNA in the lateral hypothalamus (Talley et al., 2001), where orexin neurons are clustered (Yamanaka et al., 2003). Hence, both functional and molecular data support the idea that glucose-activated channels contain TASK3 subunits. The importance of these subunits is that they determine the single-channel biophysics and anesthetic and transmitter sensitivity of K_{2P} channels, even when combined with other pore-forming subunits such as TASK1 (Kang et al., 2004; Talley and Bayliss, 2002). Here, we did not further address the nature and significance of such other subunits, although we observed binding of an antibody against TASK1 to orexin neurons (Figure 5F, n = 20 cells), which is in agreement with overlapping expression of TASK3 and TASK1 mRNA in the lateral hypothalamus (Talley et al., 2001).

Control of Orexin Cell Firing by Small Physiological Changes in Glucose Levels

As mentioned above, it is unknown whether the small changes in extracellular glucose that occur between

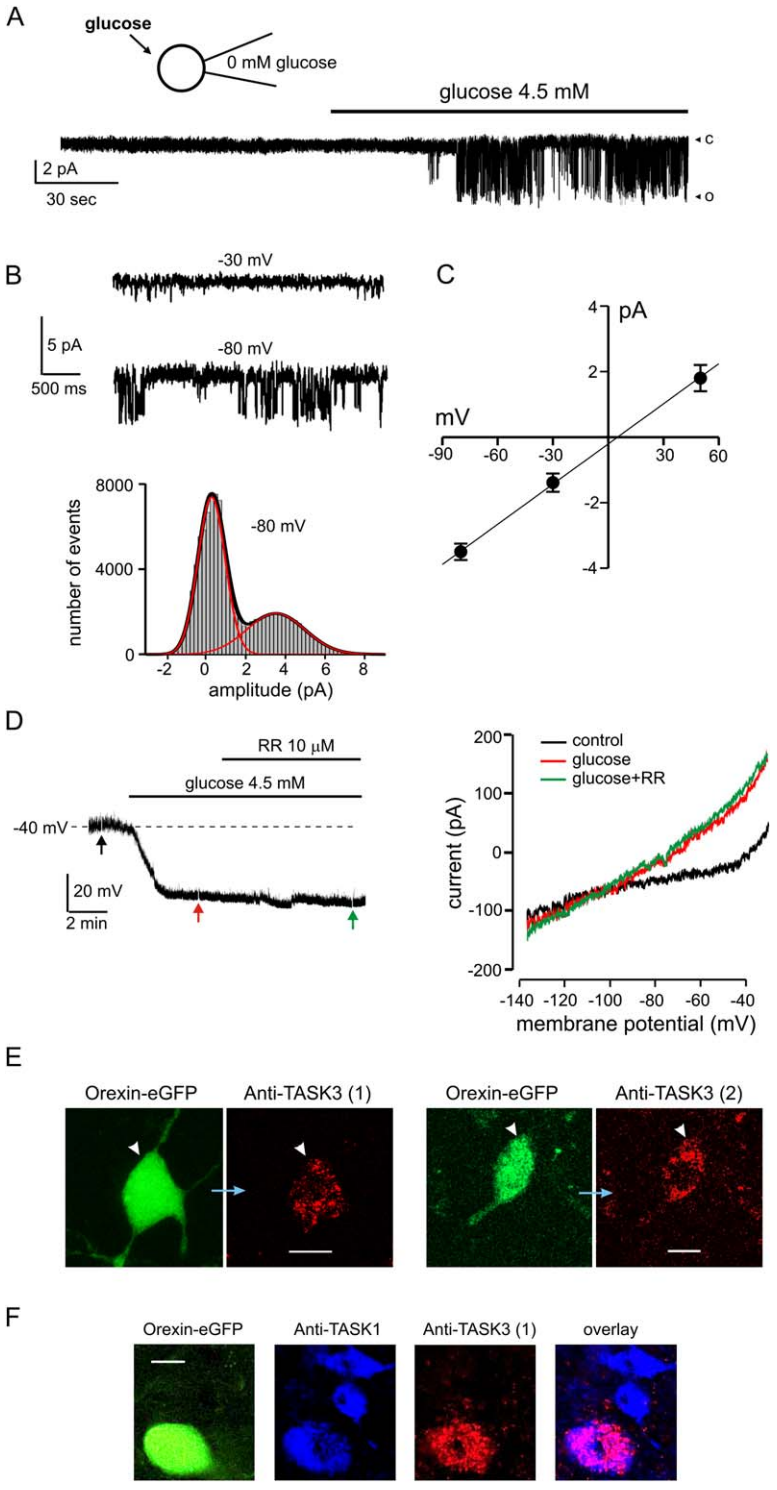

Figure 5. Properties of Glucose-Activated Channels in Orexin Neurons

(A) Cell-attached recording with no glucose in the pipette (the scheme of recording is above the trace; see Experimental Procedures for details). Closed (c) and open (o) states are indicated approximately with arrowheads. The electrode potential was zero.

(B) (Top) Cell-attached recordings of glucose-activated channels at different estimated patch potentials (see Experimental Procedures). (Bottom) Amplitude histogram of single-channel events at an estimated patch potential of −80 mV. Red lines are individual Gaussian fits; black line is the sum of these fits. Data are means ± SEM.

(C) Amplitudes of single-channel currents (determined from Gaussian fits such as that shown in [B]) at different estimated patch potentials (n = 4). The slope of the line fitted through the points is 0.04 pA/mV (40 pS).

(D) Whole-cell recording of the effect of ruthenium red (RR) on glucose-induced changes in membrane potential (left) and current (right).

(E) Detection of TASK3 proteins (red) in orexin neurons (green) with two different antibodies (Anti-TASK3 1 and 2, see Experimental Procedures). Scale bars, 10 μm.

(F) Staining of orexin neurons with an antibody against TASK1 (blue), and overlay of TASK3 staining in the same cell (colocalization is shown in pink). Scale bar, 10 μm.

Experiments performed in 1 μM tetrodotoxin.

normal meals can affect the firing rate of orexin cells. Brain interstitial glucose levels are typically 10%–30% of plasma glucose levels, and the experiments performed above involved switching between the lowest (0.2 mM) and highest (4.5 mM) extremes of brain glucose, likely to correspond to starvation and eating a very large meal, respectively (Routh, 2002; Silver and Erecinska, 1994). Variations in glucose levels in mammalian brains that occur between normal meals are much more subtle, between 1 and 2.5 mM (Routh, 2002). To provide evidence for the involvement of glucose inhibition of orexin cells in normal physiology, it is crucial to establish if their glucose-sensing machinery is sufficiently sensitive to translate such small variations in glucose into different firing rates.

Switching from 1 to 2.5 mM extracellular glucose evoked marked hyperpolarization and suppressed firing in all orexin neurons tested (Figure 6A, n = 7). The firing

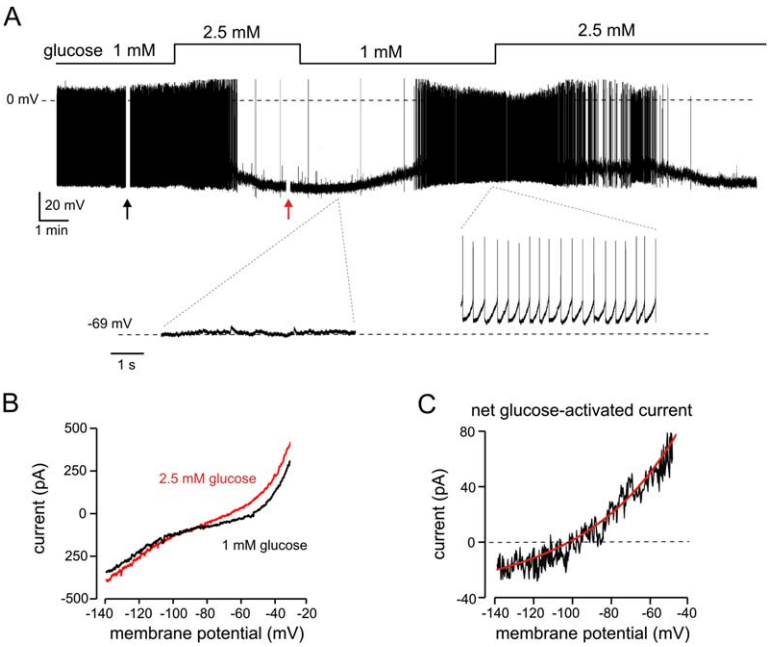

Figure 6. Sensing of Subtle Changes in Glucose Concentration by Orexin Neurons

(A) Effects of switching between 1 and 2.5 mM extracellular glucose on membrane potential. Arrows show when voltage-clamp ramps in (B) were recorded.

(B) Effects of glucose on membrane currents of the orexin neuron shown in (A).

(C) I-V relationship of net glucose-activated current in the neuron shown in (A). The red line is a fit of the GHK equation to the data.

rate decreased dramatically from 4.5 ± 1 Hz in 1 mM glucose to 0.02 ± 0.01 Hz in 2.5 mM glucose ($p < 0.001$, n = 5). The net current activated by this physiological rise in glucose showed the same properties as in the previous sections: GHK rectification and a reversal potential corresponding to E_K (−103 ± 2 mV, Figure 6B and 6C, n = 5), rapid activation, little or no inactivation, and inhibition by extracellular acid (n = 4, data not shown).

These results provide evidence that the firing rate of orexin cells is sensitive to changes in glucose that correspond to fluctuations occurring normally during the day and also show that the same electrical mechanism is involved in sensing both subtle and extreme changes in glucose.

Coupling between Extracellular Glucose and Membrane Currents

To determine whether glucose acts intracellularly or extracellularly, we applied it selectively to the inside of the cell. The rationale for this experiment is that if intracellular action of glucose is important, then increasing glucose levels inside the cell should reproduce the effects of extracellular glucose. Conversely, if glucose acts extracellularly, then intracellular glucose should neither reproduce nor prevent the effects of extracellular glucose. This is a classical experimental strategy, which was used, for example, to show that peptide hormones exert their action by acting extracellularly and not intracellularly (Philpott and Petersen, 1979). The whole-cell patch-clamp mode is a powerful and widely used way of applying chemicals inside cells, since it makes the interior of the pipette continuous with the cytosol, allowing intracellular infusion of pipette contents. Using an intracellular tracer, we previously confirmed that orexin neurons become thoroughly filled with pipette solution within 5–10 min after establishing whole-cell mode (Burdakov et al., 2005a).

To evaluate the possibility that glucose acts intracellularly, as assumed for glucose-*excited* neurons (reviewed in Burdakov et al., 2005b), we added 5 mM glucose to the pipette and dialyzed orexin cells with this solution for 10–20 min in the whole-cell mode. This neither mimicked nor prevented the electrical actions of extracellular glucose (Figures 7A and 7B, n = 6). Thus, glucose itself did not appear to act as an intracellular messenger mediating electrical inhibition of orexin neurons. Rather, its electrically important actions are mediated by action on an extracellular site (see Discussion).

We followed the same rationale to evaluate possible roles for ATP and Ca^{2+}, since these intracellular messengers can act as modulators of membrane currents (Ashcroft, 1988; Petersen et al., 1994). In all whole-cell experiments described above, the cells were already dialyzed with higher [ATP] (5 mM) than typical physiological levels in hypothalamic neurons (about 1 mM, Ainscow et al., 2002). This neither reproduced nor prevented the effects of glucose (e.g., Figure 2A). To increase ATP levels still further, we loaded cells with a supraphysiological concentration of ATP (10 mM ATP in pipette). Again, this was without effect (Figure 7C, n = 15). These results argue strongly against any dominant role for changes in cytosolic [ATP] in responses of orexin cells to glucose, consistent with recent evidence that cytosolic [ATP] is not influenced by changes in extracellular glucose in hypothalamic neurons (Ainscow et al., 2002).

Dialyzing the cells with pipette solutions containing the fast Ca^{2+} buffer BAPTA (10 mM) combined with 2 mM Ca^{2+} (to clamp cytosolic [Ca^{2+}] at ~90 nM, Mogami et al., 1998) did not prevent the electrical effects of glucose (Figure 7D, n = 15), suggesting that changes in Ca^{2+} levels are not essential for these effects. Glucose inhibition also persisted when Ca^{2+} influx into the cell was suppressed using a low Ca^{2+}/high Mg^{2+} extracellular solution (see Experimental Procedures) (Figure 7E, n = 4). These data suggest that neither Ca^{2+} entry nor Ca^{2+} mobilization from intracellular stores is critical for glucose inhibition.

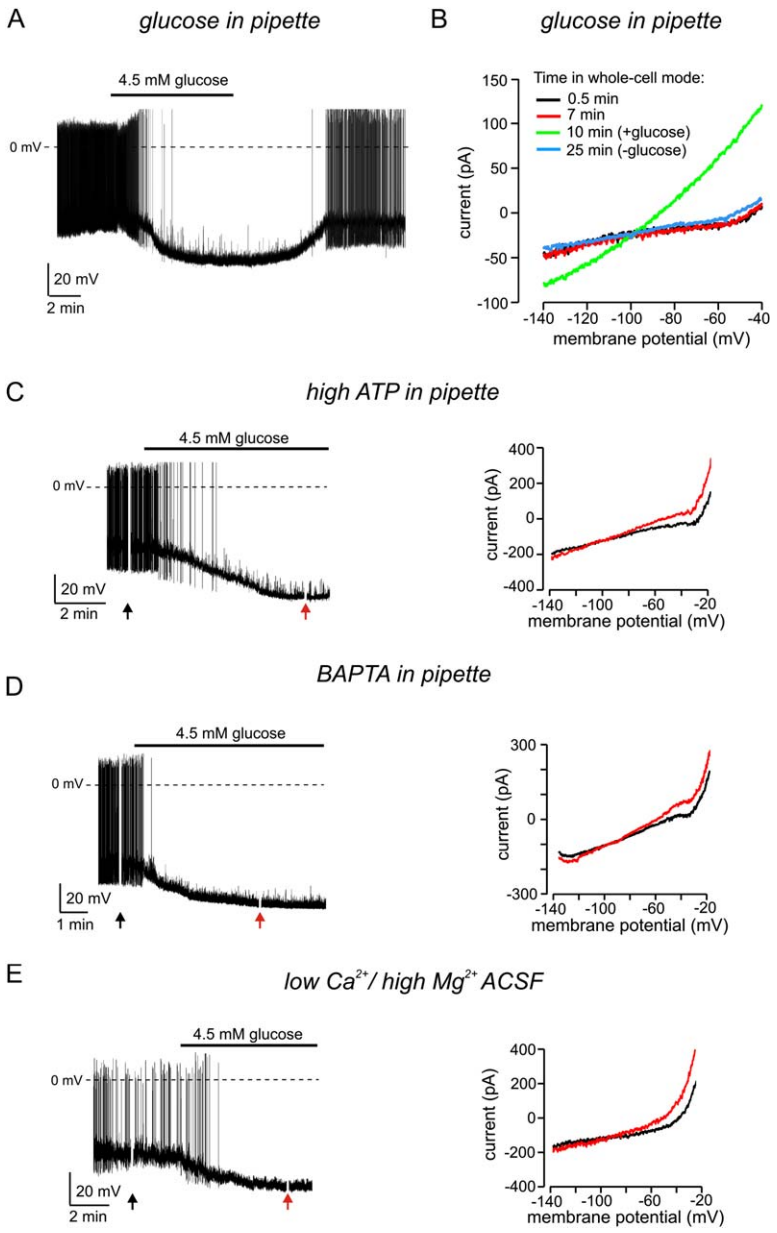

Figure 7. Effects of Putative Intracellular Messengers on Glucose Responses of Orexin Neurons

(A) Intracellular (pipette) glucose (5 mM) elicits no inhibition and does not prevent a response to extracellular glucose. The beginning of the trace corresponds to the moment when the whole-cell mode was established.

(B) Effects of intracellular and extracellular glucose on membrane I-V relationship of an orexin neuron. Five millimolar glucose was continuously present in the pipette in whole-cell mode. Extracellular glucose was elevated to 4.5 mM at 7.5 min and returned to the control value of 0.2 mM at 10.5 min.

(C) Effects of glucose on the membrane potential (left) and current (right) in a cell dialyzed with 10 mM ATP for 20 min prior to recording of the trace shown.

(D) Effects of glucose on the membrane potential (left) and current (right) in a cell dialyzed with 10 mM BAPTA/2 mM Ca^{+} for 20 min prior to recording of the trace shown. Arrows show when voltage-clamp ramps were recorded.

(E) Effects of glucose on the membrane potential (left) and current (right) in a low Ca^{2+}/ high Mg^{2+} extracellular solution.

Discussion

Despite the importance of glucose-inhibited neurons for regulation of arousal states, appetite, and metabolism, the electrical mechanism of glucose inhibition and the basic site of glucose action (intracellular versus extracellular) were unknown. Here we identify three unexpected features of glucose inhibition of orexin neurons, which control states of consciousness and metabolism. First, glucose inhibition is mediated by K_{2P} channels (Figure 2), an electrical mechanism of energy sensing that was not previously suspected in the brain or elsewhere. This identifies an important function for K_{2P} channels, a recently characterized channel family with few currently known physiological roles. Second, this electrical pathway enables orexin cells to detect fluctuations in glucose corresponding to physiological changes occurring between normal fed and fasted states (Figure 6). This provides evidence that normal daily variations in brain glucose levels can exert powerful control on the firing of orexin cells. Third, glucose acts extracellularly and not intracellularly (Figures 7A and 7B). Our results thus provide important new insights into how the brain tunes arousal and metabolism according to body energy levels.

Electrical Mechanism of Glucose Inhibition

Several K_{2P} channels are expressed in mammalian brains (Hervieu et al., 2001; Kindler et al., 2000; Medhurst et al., 2001; Talley et al., 2001), yet so far relatively few physiological roles for them have emerged. Notably, acid-sensing TASK channels in the brain stem are thought to trigger adaptive increases in arousal when brain pH falls (Bayliss et al., 2003; Talley et al., 2003). In addition, K_{2P} channels are involved in regulating excitability of cerebellar granule (Brickley et al., 2001;

Chemin et al., 2003; Millar et al., 2000), thalamocortical (Meuth et al., 2003), supraoptic (Han et al., 2003), and dorsal vagal neurons (Hopwood and Trapp, 2005), but the physiological roles of these effects remain to be elucidated. It is intriguing to uncover a role for these recently described channels in the long-elusive mechanism of glucose inhibition. Since these channels have not been previously implicated in glucose sensing or hypothalamic detection of other messengers, it would be interesting to test if they play similar roles in other glucose-inhibited cells.

In addition to GHK rectification, leak-like kinetics, and K^+ selectivity, glucose-activated currents displayed the following properties: (1) block by extracellular acid with an IC_{50} at pH 6.9 (Figure 4E), (2) potentiation by halothane (Figure 3), (3) single-channel conductance of ~40 pS (Figures 5A–5C), and (4) insensitivity to ruthenium red (Figure 5D). Together, this provides strong evidence for the involvement of heteromeric K_{2P} channels containing TASK3 subunits. Indeed, we detected TASK3 subunits in lateral hypothalamic orexin neurons using two different antibodies (Figure 5E), which is consistent with the high expression of TASK3 mRNA in this brain region (Talley et al., 2001).

However, it remains a formal possibility that other K_{2P} subunits play a role, which could be functionally similar or identical to TASK3, but are not yet fully characterized. For example, subunits that are currently thought to be nonfunctional, e.g., TASK5 (K_{2P}15.1), could play a role once activated through mechanisms similar to that recently revealed for the formerly "nonfunctional" K_{2P}1.1 (Rajan et al., 2005). Elucidating the full molecular composition of glucose-modulated K_{2P} channels is an interesting subject for future investigation; its unequivocal resolution would require manipulation of multiple KCNK genes and protein-protein interaction analyses in orexin cells.

Coupling between Extracellular Glucose and Electrical Activity

Intracellular application of glucose or ATP neither reproduced nor precluded the effects of extracellular glucose (Figures 7A–7C). Preventing cytosolic Ca^{2+} rises also had no effect on responses to glucose (Figures 7D and 7E). These data support a general mechanism of glucose sensing whereby glucose acts at an extracellular site and information is transmitted to membrane channels by an intracellular intermediary that is not ATP, Ca^{2+}, or glucose itself (Figure 8A). Traditional models by which glucose is thought to influence neuronal electrical activity involve either neuronal glucose entry and metabolism (Figure 8B) (Routh, 2002) or glial conversion of glucose to lactate (Figure 8C) (Ainscow et al., 2002; Pellerin and Magistretti, 2004). Our results provide evidence for a different mechanism in glucose-inhibited neurons (Figure 8A).

The extracellular target on which glucose acts is located on orexin neurons themselves, because they continue to sense glucose when synaptically isolated using tetrodotoxin (Figure 4A) or low extracellular Ca^{2+} (Figure 7E), as well as when studied in isolated cell preparations (Yamanaka et al., 2003). However, the appearance of glucose-activated channels in patches that do not have glucose on the extracellular side (Figures 5A and 5B) suggests that glucose does not act on the extracellular side of the channels themselves. Perhaps extracellular glucose receptors such as those identified in yeast (Holsbeeks et al., 2004) could be involved, but it is currently unknown whether similar molecules operate in mammalian brains.

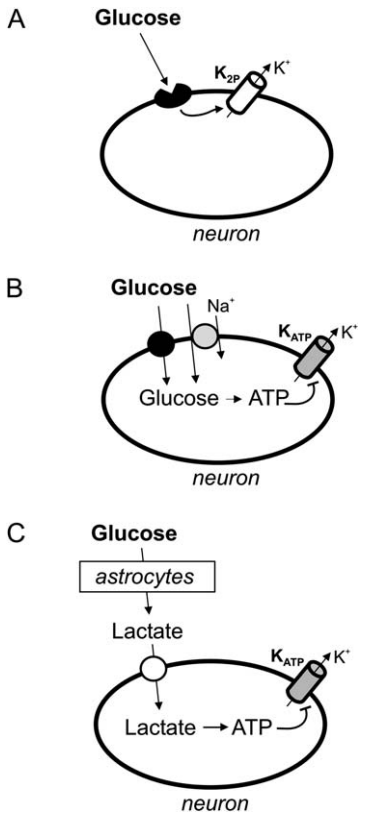

Figure 8. Schematic Cartoons of How Glucose Can Influence Electrical Activity

(A) Glucose can bind to extracellular sites and trigger intracellular transduction pathways regulating membrane channels such as K_{2P}.
(B) Glucose can enter cells via electrogenic or nonelectrogenic pathways, and be metabolized inside neurons to ATP, which inhibits plasmalemmal K_{ATP} channels.
(C) Glia (astrocytes) can convert glucose to lactate, which is then metabolized further inside neurons to produce ATP.
See Discussion for more detail.

Implications for Control of Behavioral and Metabolic States

Orexin cells are critical for promoting wakefulness and regulating metabolism and reward, and so the new mechanism of their regulation described here could contribute to these vital processes. Importantly, we demonstrate that the glucose-sensing machinery of orexin neurons is sufficiently sensitive to translate small, nonextreme, physiological fluctuations in glucose into substantial changes in firing rate (Figure 6). This raises the possibility that, besides being important for adaptive responses to starvation, modulation of orexin cells by glucose has a much wider behavioral role, contributing to the continuous daily readjustments in the level of arousal and alertness. The reversal of glucose inhibition by extracellular acid (Figure 4) may also have important

implications, because we observed this inhibition to be most pronounced (Figure 4E) within the physiological range of brain pH (6.9 to 7.4, Kintner et al., 2000). It is therefore possible that situations leading to acidification of brain interstitial space, such as an excessive reduction of breathing during sleep for example (Phillipson and Bowes, 1986), may override glucose inhibition of orexin neurons when it is necessary to increase arousal despite high energy levels.

Experimental Procedures

Generation of Transgenic Mice

Mice were made transgenic for eGFP, a red-shifted variant of the wild-type GFP that has been optimized for brighter fluorescence and higher expression in mammalian cells. Expression of eGFP was driven by the human *prepro-orexin* promoter kindly donated by Dr. Takeshi Sakurai. A 3.2 kb SacI-SalI fragment containing the 5′ flanking region and noncoding region of the *prepro-orexin* gene was excised from the construct used for the generation of human *prepro-orexin-nlacZ* transgenic mice (Sakurai et al., 1999) and cloned into the MCS of the pEGFP-1 vector (Clontech Laboratories, Inc, CA). A 4 kb SacI-AflII fragment containing the promoter and eGFP, including SV40pA signals, was excised and injected into fertilized mouse eggs from B6D2 (DBA/2xC57BL/6 F1) mice. Viable embryos were subsequently transferred to the oviducts of pseudo-pregnant B6D2 females for development to term. Transgenic offspring were identified by PCR amplification of tail DNA using primers specific for the *prepro-orexin-eGFP* sequence, and by expression of eGFP in orexin neurons (Figure 1A).

Electrophysiology

Whole-Cell Recordings

Procedures involving animals were carried out in accordance with the Animals (Scientific Procedures) Act, 1986 (UK). Coronal slices (300 μm thick) containing the lateral hypothalamus were obtained from orexin-eGFP mice (16–21 days old) as previously described (Burdakov et al., 2004). Experiments were performed at room temperature (24°C–26°C). Extracellular solution was ACSF gassed with 95% O_2 and 5% CO_2 and contained (in mM) NaCl, 125; KCl, 2.5; $MgCl_2$, 2; $CaCl_2$, 2; NaH_2PO_4, 1.2; $NaHCO_3$, 21; HEPES, 10; glucose, 0.2; pH = 7.3 with NaOH (based on brain interstitial pH in vivo, Kintner et al., 2000). ASCF [glucose] was 0.2 mM unless indicated otherwise. The small osmolarity changes associated with changing [glucose] in ASCF were either compensated with sucrose or left uncompensated; no differences were observed between the two conditions. "Low Ca^{2+}/high Mg^{2+}" ACSF contained 0.3 mM Ca^{2+} and 9 mM Mg^{2+} (Burdakov et al., 2003). Where indicated, ACSF pH was altered by addition of NaOH or HCl. "K-gluconate" intracellular (pipette) solution contained (in mM) K-gluconate, 120; KCl, 10; EGTA, 0.1; HEPES, 10; K_2ATP, 4; Na_2ATP, 1; $MgCl_2$, 2; pH = 7.3 with KOH. "KCl" intracellular solution contained (in mM) KCl, 130; EGTA, 0.1; HEPES, 10; K_2ATP, 5; NaCl, 1; $MgCl_2$, 2; pH = 7.3 with KOH. All the chemicals were from Sigma.

Neurons were visualized using an Olympus BX50WI upright microscope equipped with infrared gradient contrast optics (Dodt et al., 2002), a mercury lamp, and filters for visualizing eGFP-containing cells. Current- and voltage-clamp whole-cell recordings were performed using an EPC-9 amplifier (Heka, Lambrecht, Germany). In current-clamp experiments, the holding current was zero unless indicated otherwise. Patch pipettes were pulled from borosilicate glass and had tip resistances of 2–3 MΩ when filled with the "KCl" pipette solution. Series resistances were in the range of 5–8 MΩ and were not compensated. Data were sampled and filtered using Pulse/Pulsefit software (Heka, Lambrecht, Germany) and analyzed with Pulsefit and Origin (Microcal, Northampton, MA) software. Steady-state membrane I-V relationships (Figure 2C) were obtained using 500 ms long hyperpolarizing and depolarizing voltage-clamp steps from a holding potential of −90 mV. Alternatively, I-Vs were obtained by ramping the membrane potential from 0 to −140 mV at a rate of 0.1 mV/ms, which was sufficiently slow to allow the K^+ current to reach steady state at each potential (Meuth et al., 2003). Data are given as mean ± SEM.

Where indicated, I-Vs were fitted with the Goldman-Hodgkin-Katz (GHK) current equation (Hille, 2001), in the following form:

$$I = P_K z^2 \frac{VF^2}{RT} \frac{[K^+]_i - [K^+]_o \exp(-zFV/RT)}{1 - \exp(-zFV/RT)}$$

Here, I is current, V is membrane potential, z is the charge of a potassium ion (+1), $[K^+]_i$ is the pipette K^+ concentration, $[K^+]_o$ is the ACSF K^+ concentration, T is temperature (298.15 K, corresponding to 25°C), and R and F have their usual meanings (Hille, 2001). P_K (a constant reflecting the K^+ permeability of the membrane) was the only free parameter during fits. The values of P_K used to obtain the fits shown were 0.0176 (Figure 2C), 0.03485 (Figure 3B), 0.0439 (Figure 4D), and 0.0202 (Figure 6C).

Dose-response relation for acid-induced inhibition of glucose-activated current (I) was fitted with a modified Hill equation:

$$I = I_{max} - I_{max} \frac{[H^+]^h}{IC_{50}^h + [H^+]^h}$$

Here, I_{max} is the maximal current, $[H^+]$ is the extracellular proton concentration, IC_{50} is the value of $[H^+]$ at which the inhibition is half-maximal, and h is the Hill coefficient. The fit shown in Figure 4E was obtained with the following parameters: I_{max} = 171 pA, h = 1.2, IC_{50} = 127 nM (equivalent to pH of 6.9).

Single-Channel Recordings

For cell-attached recordings from cell bodies of orexin neurons, patch-pipettes were filled with a high K^+ solution containing (in mM) KCl 120, EGTA 11, $CaCl_2$ 1, $MgCl_2$ 2, HEPES 10, adjusted to pH 7.25 with 35 mM KOH (final K^+ concentration 155 mM) (Verheugen et al., 1999). In neurons, using this solution results in sufficiently symmetrical K^+ concentrations on the two sides of the cell-attached patch to justify the assumption that E_K in the patch is ≈ 0 mV (Verheugen et al., 1999). When the membrane potential is negative and the electrode potential is zero, K^+ currents thus appear as inward currents (Figures 5A and 5B). Data were sampled at 10 kHz and filtered at 3 kHz. All other experimental conditions were the same as for whole-cell recordings. Only patches with no channel activity in control (0.2 mM glucose) ASCF were used for further experimentation, and channel amplitudes were determined in patches judged to contain one glucose-activated channel. Estimated values of the patch potential (obtained as in Verheugen et al., 1999) were in close agreement with whole-cell data: 10 min after applying 4.5 mM glucose, patch and whole-cell potentials were −80 ± 3 mV and −81 ± 2 mV, respectively (n = 4 cells for each case). Single-channel conductances were calculated from slopes of linear fits (Origin) of channel I-V relationships (Figure 5C). We also performed cell-attached recordings of glucose-activated channels using pipette solution from Kang et al. (2004), which yielded similar channel conductances (38 ± 2 pS, n = 3 patches, data not shown).

Immunocytochemistry and Confocal Imaging

Immunolabeling for orexin-A was performed as in our previous studies (Burdakov et al., 2004, 2005a). For detection of K_{2P} proteins, the brains of orexin-eGFP mice were fixed in 4% PFA at 4°C for 24 hr and then cut in PBS into 150–200 μm coronal sections. Slices were incubated for 20 min in a blocking medium containing 10% horse serum, 0.2% BSA, and 0.5% Triton in PBS, followed by two washes in PBS. For detection of TASK3 we used two different antibodies. Antibody (1) in Figure 5E was a goat polyclonal antibody (Rusznak et al., 2004; Yamamoto and Taniguchi, 2003) raised against a peptide mapping to the C terminus of TASK3 of rat origin (1:100, Santa Cruz Biotechnology, CA). Antibody (2) in Figure 5E was a rabbit polyclonal antibody raised against an epitope corresponding to residues 57–73 of the rat TASK3 protein (1:1000, Alomone labs, Israel). The antibody against TASK1 (Figure 5F) was a rabbit polyclonal antibody (Kindler et al., 2000; Lopes et al., 2000; Millar et al., 2000) raised against the peptide (C)EDEK RDAEH RALLT RNGQ corresponding to residues 252–269 of human TASK1 (1:1000, Alomone Labs, Jerusalem, Israel). Slices were incubated with the primary antibodies overnight in PBS containing 1% horse serum, 0.2% BSA, and 0.5% Triton, followed by four washes in PBS. Subsequently, slices were incubated with secondary antibodies, chicken antirabbit IgG-Alexa Fluor 647 (1:1000,

Molecular Probes, Eugene, Oregon) and donkey antigoat IgG-Texas red (1:200, Santa Cruz Biotechnology), for 90 min in PBS containing 0.2% BSA and 0.5% Triton, followed by six washes in PBS. Slices were then mounted on glass coverslips in Vectashield antibleach mounting medium (Vector Laboratories, Peterborough, UK). For negative controls, the primary antibodies were preincubated for 1 hr with control peptide antigens (1 μg of antigen per 1 μg of antibody) provided with the antibodies. All the chemicals were from Sigma unless stated otherwise. Slices were analyzed using a Leica Microsystems TCS SL confocal laser-scanning microscope (Mannheim, Germany). eGFP, Texas red, and Alexa Fluor 647 were excited at 477 nm, 543 nm, and 633 nm, respectively, and emission was detected at 490–550 nm, 570–620 nm, and 660–740 nm, respectively. For optimal separation of fluorescent signals, the sequential "between lines" scanning mode of the microscope was used.

Acknowledgments

D.B. (independent principal investigator holding a Royal Society Dorothy Hodgkin Fellowship) initiated, designed, and directed this study and wrote the text. L.F. and L.J. generated and supplied the orexin-eGFP transgenic mice. H.A. (supported by a Wellcome Trust OXION Training Fellowship) and R.W. (supported by a BBSRC PhD studentship) contributed to immunocytochemical experiments. A.V. and the University of Manchester provided most of the experimental facilities. Electrophysiological experiments were performed by D.B. We thank Nick Willcox and Christina Riggs for advice on the text.

Received: October 28, 2005
Revised: February 9, 2006
Accepted: April 28, 2006
Published: May 31, 2006

References

Ainscow, E.K., Mirshamsi, S., Tang, T., Ashford, M.L., and Rutter, G.A. (2002). Dynamic imaging of free cytosolic ATP concentration during fuel sensing by rat hypothalamic neurones: evidence for ATP-independent control of ATP-sensitive K(+) channels. J. Physiol. *544*, 429–445.

Anand, B.K., Chhina, G.S., Sharma, K.N., Dua, S., and Singh, B. (1964). Activity of single neurons in the hypothalamic feeding centers: effect of glucose. Am. J. Physiol. *207*, 1146–1154.

Ashcroft, F.M. (1988). Adenosine 5′-triphosphate-sensitive potassium channels. Annu. Rev. Neurosci. *11*, 97–118.

Ashford, M.L., Boden, P.R., and Treherne, J.M. (1990). Glucose-induced excitation of hypothalamic neurones is mediated by ATP-sensitive K+ channels. Pflugers Arch. *415*, 479–483.

Bayliss, D.A., Sirois, J.E., and Talley, E.M. (2003). The TASK family: two-pore domain background K+ channels. Mol. Interv. *3*, 205–219.

Berg, A.P., Talley, E.M., Manger, J.P., and Bayliss, D.A. (2004). Motoneurons express heteromeric TWIK-related acid-sensitive K+ (TASK) channels containing TASK-1 (KCNK3) and TASK-3 (KCNK9) subunits. J. Neurosci. *24*, 6693–6702.

Borgland, S.L., Taha, S.A., Sarti, F., Fields, H.L., and Bonci, A. (2006). Orexin A in the VTA is critical for the induction of synaptic plasticity and behavioral sensitization to cocaine. Neuron *49*, 589–601.

Brickley, S.G., Revilla, V., Cull-Candy, S.G., Wisden, W., and Farrant, M. (2001). Adaptive regulation of neuronal excitability by a voltage-independent potassium conductance. Nature *409*, 88–92.

Burdakov, D., Liss, B., and Ashcroft, F.M. (2003). Orexin excites GABAergic neurons of the arcuate nucleus by activating the sodium-calcium exchanger. J. Neurosci. *23*, 4951–4957.

Burdakov, D., Alexopoulos, H., Vincent, A., and Ashcroft, F.M. (2004). Low-voltage-activated A-current controls the firing dynamics of mouse hypothalamic orexin neurons. Eur. J. Neurosci. *20*, 3281–3285.

Burdakov, D., Gerasimenko, O., and Verkhratsky, A. (2005a). Physiological changes in glucose differentially modulate the excitability of hypothalamic melanin-concentrating hormone and orexin neurons in situ. J. Neurosci. *25*, 2429–2433.

Burdakov, D., Luckman, S.M., and Verkhratsky, A. (2005b). Glucose-sensing neurons of the hypothalamus. Philos. Trans. R. Soc. Lond. B Biol. Sci. *360*, 2227–2235.

Chemelli, R.M., Willie, J.T., Sinton, C.M., Elmquist, J.K., Scammell, T., Lee, C., Richardson, J.A., Williams, S.C., Xiong, Y., Kisanuki, Y., et al. (1999). Narcolepsy in orexin knockout mice: molecular genetics of sleep regulation. Cell *98*, 437–451.

Chemin, J., Girard, C., Duprat, F., Lesage, F., Romey, G., and Lazdunski, M. (2003). Mechanisms underlying excitatory effects of group I metabotropic glutamate receptors via inhibition of 2P domain K+ channels. EMBO J. *22*, 5403–5411.

Czirjak, G., and Enyedi, P. (2002). Formation of functional heterodimers between the TASK-1 and TASK-3 two-pore domain potassium channel subunits. J. Biol. Chem. *277*, 5426–5432.

de Lecea, L., Kilduff, T.S., Peyron, C., Gao, X., Foye, P.E., Danielson, P.E., Fukuhara, C., Battenberg, E.L., Gautvik, V.T., Bartlett, F.S., 2nd.., et al. (1998). The hypocretins: hypothalamus-specific peptides with neuroexcitatory activity. Proc. Natl. Acad. Sci. USA *95*, 322–327.

Dodt, H.U., Eder, M., Schierloh, A., and Zieglgansberger, W. (2002). Infrared-guided laser stimulation of neurons in brain slices. Sci. STKE.http://stke.sciencemag.org/cgi/content/full/OC_sigtrans;2002/120/pl2.

Goldstein, S.A., Bockenhauer, D., O'Kelly, I., and Zilberberg, N. (2001). Potassium leak channels and the KCNK family of two-P-domain subunits. Nat. Rev. Neurosci. *2*, 175–184.

Goldstein, S.A., Bayliss, D.A., Kim, D., Lesage, F., Plant, L.D., and Rajan, S. (2005). International Union of Pharmacology. LV. Nomenclature and molecular relationships of two-P potassium channels. Pharmacol. Rev. *57*, 527–540.

Gribkoff, V.K., Starrett, J.E., Jr., and Dworetzky, S.I. (2001). Maxi-K potassium channels: form, function, and modulation of a class of endogenous regulators of intracellular calcium. Neuroscientist *7*, 166–177.

Han, J., Gnatenco, C., Sladek, C.D., and Kim, D. (2003). Background and tandem-pore potassium channels in magnocellular neurosecretory cells of the rat supraoptic nucleus. J. Physiol. *546*, 625–639.

Hara, J., Beuckmann, C.T., Nambu, T., Willie, J.T., Chemelli, R.M., Sinton, C.M., Sugiyama, F., Yagami, K., Goto, K., Yanagisawa, M., and Sakurai, T. (2001). Genetic ablation of orexin neurons in mice results in narcolepsy, hypophagia, and obesity. Neuron *30*, 345–354.

Harris, G.C., Wimmer, M., and Aston-Jones, G. (2005). A role for lateral hypothalamic orexin neurons in reward seeking. Nature *437*, 556–559.

Hervieu, G.J., Cluderay, J.E., Gray, C.W., Green, P.J., Ranson, J.L., Randall, A.D., and Meadows, H.J. (2001). Distribution and expression of TREK-1, a two-pore-domain potassium channel, in the adult rat CNS. Neuroscience *103*, 899–919.

Hille, B. (2001). Ion Channels of Excitable Membranes, Third Edition (Sunderland, MA: Sinauer Associates, Inc.).

Holsbeeks, I., Lagatie, O., Van Nuland, A., Van de Velde, S., and Thevelein, J.M. (2004). The eukaryotic plasma membrane as a nutrient-sensing device. Trends Biochem. Sci. *29*, 556–564.

Hopwood, S.E., and Trapp, S. (2005). TASK-like K+ channels mediate effects of 5-HT and extracellular pH in rat dorsal vagal neurones in vitro. J. Physiol. *568*, 145–154.

Kang, D., Han, J., Talley, E.M., Bayliss, D.A., and Kim, D. (2004). Functional expression of TASK-1/TASK-3 heteromers in cerebellar granule cells. J. Physiol. *554*, 64–77.

Kindler, C.H., Pietruck, C., Yost, C.S., Sampson, E.R., and Gray, A.T. (2000). Localization of the tandem pore domain K+ channel TASK-1 in the rat central nervous system. Brain Res. Mol. Brain Res. *80*, 99–108.

Kintner, D.B., Anderson, M.K., Fitzpatrick, J.H., Jr., Sailor, K.A., and Gilboe, D.D. (2000). 31P-MRS-based determination of brain intracellular and interstitial pH: its application to in vivo H+ compartmentation and cellular regulation during hypoxic/ischemic conditions. Neurochem. Res. *25*, 1385–1396.

Leonoudakis, D., Gray, A.T., Winegar, B.D., Kindler, C.H., Harada, M., Taylor, D.M., Chavez, R.A., Forsayeth, J.R., and Yost, C.S.

(1998). An open rectifier potassium channel with two pore domains in tandem cloned from rat cerebellum. J. Neurosci. *18*, 868–877.

Lesage, F., and Lazdunski, M. (2000). Molecular and functional properties of two-pore-domain potassium channels. Am. J. Physiol. Renal Physiol. *279*, F793–F801.

Levin, B.E., Dunn-Meynell, A.A., and Routh, V.H. (1999). Brain glucose sensing and body energy homeostasis: role in obesity and diabetes. Am. J. Physiol. *276*, R1223–R1231.

Li, Y., Gao, X.B., Sakurai, T., and van den Pol, A.N. (2002). Hypocretin/Orexin excites hypocretin neurons via a local glutamate neuron-A potential mechanism for orchestrating the hypothalamic arousal system. Neuron *36*, 1169–1181.

Lin, L., Faraco, J., Li, R., Kadotani, H., Rogers, W., Lin, X., Qiu, X., de Jong, P.J., Nishino, S., and Mignot, E. (1999). The sleep disorder canine narcolepsy is caused by a mutation in the hypocretin (orexin) receptor 2 gene. Cell *98*, 365–376.

Lopes, C.M., Gallagher, P.G., Buck, M.E., Butler, M.H., and Goldstein, S.A. (2000). Proton block and voltage gating are potassium-dependent in the cardiac leak channel Kcnk3. J. Biol. Chem. *275*, 16969–16978.

Marcus, J.N., Aschkenasi, C.J., Lee, C.E., Chemelli, R.M., Saper, C.B., Yanagisawa, M., and Elmquist, J.K. (2001). Differential expression of orexin receptors 1 and 2 in the rat brain. J. Comp. Neurol. *435*, 6–25.

Medhurst, A.D., Rennie, G., Chapman, C.G., Meadows, H., Duckworth, M.D., Kelsell, R.E., Gloger, I.I., and Pangalos, M.N. (2001). Distribution analysis of human two pore domain potassium channels in tissues of the central nervous system and periphery. Brain Res. Mol. Brain Res. *86*, 101–114.

Meuth, S.G., Budde, T., Kanyshkova, T., Broicher, T., Munsch, T., and Pape, H.C. (2003). Contribution of TWIK-related acid-sensitive K+ channel 1 (TASK1) and TASK3 channels to the control of activity modes in thalamocortical neurons. J. Neurosci. *23*, 6460–6469.

Millar, J.A., Barratt, L., Southan, A.P., Page, K.M., Fyffe, R.E., Robertson, B., and Mathie, A. (2000). A functional role for the two-pore domain potassium channel TASK-1 in cerebellar granule neurons. Proc. Natl. Acad. Sci. USA *97*, 3614–3618.

Mogami, H., Tepikin, A.V., and Petersen, O.H. (1998). Termination of cytosolic Ca2+ signals: Ca2+ reuptake into intracellular stores is regulated by the free Ca2+ concentration in the store lumen. EMBO J. *17*, 435–442.

O'Connell, A.D., Morton, M.J., and Hunter, M. (2002). Two-pore domain K+ channels-molecular sensors. Biochim. Biophys. Acta *1566*, 152–161.

Oomura, Y., Ono, T., Ooyama, H., and Wayner, M.J. (1969). Glucose and osmosensitive neurones of the rat hypothalamus. Nature *222*, 282–284.

Oomura, Y., Ooyama, H., Sugimori, M., Nakamura, T., and Yamada, Y. (1974). Glucose inhibition of the glucose-sensitive neurone in the rat lateral hypothalamus. Nature *247*, 284–286.

Patel, A.J., and Honore, E. (2001). Properties and modulation of mammalian 2P domain K+ channels. Trends Neurosci. *24*, 339–346.

Pellerin, L., and Magistretti, P.J. (2004). Neuroenergetics: calling upon astrocytes to satisfy hungry neurons. Neuroscientist *10*, 53–62.

Petersen, O.H., Petersen, C.C., and Kasai, H. (1994). Calcium and hormone action. Annu. Rev. Physiol. *56*, 297–319.

Peyron, C., Tighe, D.K., van den Pol, A.N., de Lecea, L., Heller, H.C., Sutcliffe, J.G., and Kilduff, T.S. (1998). Neurons containing hypocretin (orexin) project to multiple neuronal systems. J. Neurosci. *18*, 9996–10015.

Peyron, C., Faraco, J., Rogers, W., Ripley, B., Overeem, S., Charnay, Y., Nevsimalova, S., Aldrich, M., Reynolds, D., Albin, R., et al. (2000). A mutation in a case of early onset narcolepsy and a generalized absence of hypocretin peptides in human narcoleptic brains. Nat. Med. *6*, 991–997.

Phillipson, E., and Bowes, G. (1986). Control of breathing during sleep. In Handbook of Physiology: The Respiratory System (Bethesda, MD: American Physiological Society), pp. 649–689.

Philpott, H.G., and Petersen, O.H. (1979). Extracellular but not intracellular application of peptide hormones activates pancreatic acinar cells. Nature *281*, 684–686.

Rajan, S., Wischmeyer, E., Xin Liu, G., Preisig-Muller, R., Daut, J., Karschin, A., and Derst, C. (2000). TASK-3, a novel tandem pore domain acid-sensitive K+ channel. An extracellular histiding as pH sensor. J. Biol. Chem. *275*, 16650–16657.

Rajan, S., Plant, L.D., Rabin, M.L., Butler, M.H., and Goldstein, S.A. (2005). Sumoylation silences the plasma membrane leak K+ channel K2P1. Cell *121*, 37–47.

Routh, V.H. (2002). Glucose-sensing neurons: are they physiologically relevant? Physiol. Behav. *76*, 403–413.

Rusznak, Z., Pocsai, K., Kovacs, I., Por, A., Pal, B., Biro, T., and Szucs, G. (2004). Differential distribution of TASK-1, TASK-2 and TASK-3 immunoreactivities in the rat and human cerebellum. Cell. Mol. Life Sci. *61*, 1532–1542.

Sakurai, T., Amemiya, A., Ishii, M., Matsuzaki, I., Chemelli, R.M., Tanaka, H., Williams, S.C., Richardson, J.A., Kozlowski, G.P., Wilson, S., et al. (1998). Orexins and orexin receptors: a family of hypothalamic neuropeptides and G protein-coupled receptors that regulate feeding behavior. Cell *92*, 573–585.

Sakurai, T., Moriguchi, T., Furuya, K., Kajiwara, N., Nakamura, T., Yanagisawa, M., and Goto, K. (1999). Structure and function of human prepro-orexin gene. J. Biol. Chem. *274*, 17771–17776.

Saper, C.B., Chou, T.C., and Elmquist, J.K. (2002). The need to feed: homeostatic and hedonic control of eating. Neuron *36*, 199–211.

Schwartz, M.W., Woods, S.C., Porte, D., Jr., Seeley, R.J., and Baskin, D.G. (2000). Central nervous system control of food intake. Nature *404*, 661–671.

Selbach, O., Doreulee, N., Bohla, C., Eriksson, K.S., Sergeeva, O.A., Poelchen, W., Brown, R.E., and Haas, H.L. (2004). Orexins/hypocretins cause sharp wave- and theta-related synaptic plasticity in the hippocampus via glutamatergic, gabaergic, noradrenergic, and cholinergic signaling. Neuroscience *127*, 519–528.

Silver, I.A., and Erecinska, M. (1994). Extracellular glucose concentration in mammalian brain: continuous monitoring of changes during increased neuronal activity and upon limitation in oxygen supply in normo-, hypo-, and hyperglycemic animals. J. Neurosci. *14*, 5068–5076.

Sirois, J.E., Lei, Q., Talley, E.M., Lynch, C., 3rd., and Bayliss, D.A. (2000). The TASK-1 two-pore domain K+ channel is a molecular substrate for neuronal effects of inhalation anesthetics. J. Neurosci. *20*, 6347–6354.

Smith, H.R., and Pang, K.C. (2005). Orexin-saporin lesions of the medial septum impair spatial memory. Neuroscience *132*, 261–271.

Sutcliffe, J.G., and de Lecea, L. (2002). The hypocretins: setting the arousal threshold. Nat. Rev. Neurosci. *3*, 339–349.

Talley, E.M., and Bayliss, D.A. (2002). Modulation of TASK-1 (Kcnk3) and TASK-3 (Kcnk9) potassium channels: volatile anesthetics and neurotransmitters share a molecular site of action. J. Biol. Chem. *277*, 17733–17742.

Talley, E.M., Solorzano, G., Lei, Q., Kim, D., and Bayliss, D.A. (2001). Cns distribution of members of the two-pore-domain (KCNK) potassium channel family. J. Neurosci. *21*, 7491–7505.

Talley, E.M., Sirois, J.E., Lei, Q., and Bayliss, D.A. (2003). Two-pore-Domain (KCNK) potassium channels: dynamic roles in neuronal function. Neuroscientist *9*, 46–56.

Thannickal, T.C., Moore, R.Y., Nienhuis, R., Ramanathan, L., Gulyani, S., Aldrich, M., Cornford, M., and Siegel, J.M. (2000). Reduced number of hypocretin neurons in human narcolepsy. Neuron *27*, 469–474.

Verheugen, J.A., Fricker, D., and Miles, R. (1999). Noninvasive measurements of the membrane potential and GABAergic action in hippocampal interneurons. J. Neurosci. *19*, 2546–2555.

Willie, J.T., Chemelli, R.M., Sinton, C.M., and Yanagisawa, M. (2001). To eat or to sleep? Orexin in the regulation of feeding and wakefulness. Annu. Rev. Neurosci. *24*, 429–458.

Yamamoto, Y., and Taniguchi, K. (2003). Heterogeneous expression of TASK-3 and TRAAK in rat paraganglionic cells. Histochem. Cell Biol. *120*, 335–339.

Yamanaka, A., Beuckmann, C.T., Willie, J.T., Hara, J., Tsujino, N., Mieda, M., Tominaga, M., Yagami, K., Sugiyama, F., Goto, K., et al. (2003). Hypothalamic orexin neurons regulate arousal according to energy balance in mice. Neuron *38*, 701–713.